

# Discrete singular convolution and its application to the analysis of plates with internal supports. Part 1: Theory and algorithm

G. W. Wei<sup>1,2,\*</sup>, Y. B. Zhao<sup>1</sup> and Y. Xiang<sup>3</sup>

<sup>1</sup>*Department of Computational Science, National University of Singapore, Singapore 117543, Singapore*

<sup>2</sup>*Department of Mathematics, Michigan State University, East Lansing, MI 28824, U.S.A.*

<sup>3</sup>*School of Engineering and Industrial Design, University of Western Sydney, Penrith South DC NSW 1797, Australia*

## SUMMARY

This paper presents a novel computational approach, the discrete singular convolution (DSC) algorithm, for analysing plate structures. The basic philosophy behind the DSC algorithm for the approximation of functions and their derivatives is studied. Approximations to the delta distribution are constructed as either bandlimited reproducing kernels or approximate reproducing kernels. Unified features of the DSC algorithm for solving differential equations are explored. It is demonstrated that different methods of implementation for the present algorithm, such as global, local, Galerkin, collocation, and finite difference, can be deduced from a single starting point. The use of the algorithm for the vibration analysis of plates with internal supports is discussed. Detailed formulation is given to the treatment of different plate boundary conditions, including simply supported, elastically supported and clamped edges. This work paves the way for applying the DSC approach in the following paper to plates with complex support conditions, which have not been fully addressed in the literature yet. Copyright © 2002 John Wiley & Sons, Ltd.

KEY WORDS: square plates; vibration analysis; wavelets; discrete singular convolution

## 1. INTRODUCTION

Plate, beam and shell are omnipresent in modern science and engineering. Whether the concern is with aircraft and missile surface components, reinforced concrete floor slabs, glass-window panes, electric circuit boards, cellular phones or certain layered geological formations, engineers and scientists are frequently called upon to predict the natural frequencies, bending stresses and buckling loads of elastic beams, plates and shells. To achieve these goals, one is

---

\*Correspondence to: G. W. Wei, Department of Mathematics, Michigan State University, East Lansing, MI 28824, U.S.A.

†E-mail: cscweigw@nus.edu.sg

Contract grant sponsor: National University of Singapore

Contract grant sponsor: University of Western Sydney

required to have thorough knowledge of the fundamental equations of beams, plates and shells as well as an excellent understanding of various methods of solution. Since analytical solution can only be available to a few limited cases, computer simulation is the major approach for the theoretical analysis for most of the above mentioned practical engineering structures. The study on vibration of plates is one of the most important research areas in civil, mechanical and aerospace engineering. The pioneer study in this area is credited to Chladni [1] who observed the nodal patterns on square plates at their resonant frequencies. Extensive studies on vibration of plates have been conducted since then and the publications have been well documented in a series of review papers [2–7] and books [8, 9]. The level of difficulty in obtaining solutions is greatly increased when a structure, such as a plate, involves partial internal supports [10–25].

There has been a great deal of achievement in numerical methodology for the analyses of beams and plates in the past few decades. Both global methods and local methods are very successful in structural mechanics applications. Global methods are highly accurate. But local methods are more flexible in handling complex geometries, boundary conditions and internal supports. There are problems in the practical applications requiring both the high computational accuracy and the flexibility in handling complex geometries, boundary conditions and internal supports. One such problem is the analysis of the vibration response of an airplane surface under high frequency disturbance. It is a common approach for mechanical fatigue analysis and metal crack detection. It is desirable to have a computational method that combines the high accuracy of a global method with the flexibility of a local method for science and engineering applications.

The discrete singular convolution (DSC) algorithm [26–29] was developed for filling this gap. Sequences of approximations to the singular kernels of Hilbert type, Abel type and delta type were constructed. Applications were discussed to analytical signal processing, Radon transform and surface interpolation. The mathematical foundation of the DSC algorithm is the theory of distributions [30] and the theory of wavelets. Numerical solutions to differential equations are formulated via the singular kernels of delta type. By appropriately selecting parameters in the DSC kernel, the DSC approach exhibits controllable accuracy for integration and shows excellent flexibility in handling complex geometries and boundary conditions. It was demonstrated [27] that different implementations of the DSC algorithm, such as global, local, Galerkin, collocation, and finite difference, can be deduced from a single starting point. Thus, the DSC algorithm provides a unified representation to these numerical methods. Many DSC kernels, such as the (regularized) Shannon delta sequence kernel, the (regularized) Dirichlet delta sequence kernel, the (regularized) Lagrange delta sequence kernel and the (regularized) de la Vallée Poussin delta sequence kernel, have been constructed [26]. Practical applications were examined for the numerical solution of the Fokker–Planck equation [26, 27] and for the Schrödinger equation [31]. Another development in the application of the DSC algorithm is its use in computing numerical solutions of the Navier–Stokes equation [29, 32] and in structural analysis [33, 34]. In the context of image processing, DSC kernels were used to facilitate a new anisotropic diffusion operator for image restoration from noise [35]. Most recently, the DSC algorithm was used to resolve a few numerically challenging problems. It was utilized to integrate the (non-linear) sine-Gordon equation with the initial values close to a homoclinic manifold singularity [36], for which conventional local methods encounter great difficulties and result in numerically induced chaos [37]. Another difficult example resolved by using the DSC algorithm

is the integration of the (non-linear) Cahn–Hilliard equation in a circular domain, which is challenging because of the fourth order artificial singularity at the origin and the complex phase space geometry [38].

The purpose of this paper is to study the computational philosophy of the DSC algorithm and to introduce the algorithm for vibration analysis of plates with internal supports. For the purpose of numerical computation, both bandlimited reproducing kernels and approximate reproducing kernels are discussed as sequences of approximations to the universal reproducing kernel, the delta distribution. A systematic treatment is proposed for handling a general class of boundary conditions. We explore the unified features of the DSC algorithm for numerical approximation of differential equations. It is found that several conventional computational methods, such as methods of global, local, Galerkin, collocation, and finite difference can be derived from a single starting point. In particular, a Galerkin-induced collocation algorithm is discussed. A set of generalized finite difference schemes are shown to exhibit global-finite difference features at certain limit of DSC parameters.

The present study on vibration of rectangular plates with internal supports is presented in a series of two papers. Part 1 of the series presents the DSC approach in general. A number of new DSC kernels are constructed as approximations to the universal reproducing kernel—the delta distribution. Approximation of functions and their derivatives is discussed. The unified features of the DSC algorithm are explored in the framework of the method of weighted residuals. The implementation of the proposed algorithm to analysis of plates is explored. In particular, due to the presence of fourth order derivatives in the governing partial differential equations, structural analysis requires the treatment of complex boundary conditions. Such a treatment is studied in a systematic manner. Part 2 of the series presents the vibration analysis of square plates with partial internal straight line supports and complex internal supports under various combinations of boundary conditions.

The organization of the paper is as follows. In Section 2, we study the computational philosophy of the DSC algorithm. The DSC analysis of plate vibrations is presented in Section 3. A systematic treatment of boundary conditions is proposed for being used in implicit schemes. This paper ends with a conclusion.

## 2. THE DISCRETE SINGULAR CONVOLUTION

The philosophy of the DSC algorithm is studied in this section. The mathematical foundation is discussed. A number of new kernels are constructed. Wavelet analysis of the algorithm is given. Numerical applications to partial differential equations are formulated in terms of the method of weighted residuals.

### 2.1. *Approximation of singular convolution*

Singular convolutions (SC) are a special class of mathematical transformations, which appear in many science and engineering problems, such as Hilbert transform, Abel transform and Radon transform. It is most convenient to discuss the singular convolution in the context of the theory of distributions. The latter has a significant impact in mathematical analysis. Not only it provides a rigorous justification for a number of informal manipulations in physical and engineering sciences, but also it opens a new area of mathematics, which in turn

gives impetus to many other mathematical disciplines, such as operator calculus, differential equations, functional analysis, harmonic analysis and transformation theory. In fact, the theory of wavelets and frames, a new mathematical branch developed in recent years, can also find its root in the theory of distributions.

Let  $T$  be a distribution and  $\eta(t)$  be an element of the space of test functions. A singular convolution is defined as

$$F(t) = (T * \eta)(t) = \int_{-\infty}^{\infty} T(t-x)\eta(x) dx \quad (1)$$

Here  $T(t-x)$  is a singular kernel. Depending on the form of the kernel  $T$ , the singular convolution is the central issue for a wide range of science and engineering problems. For example, the singular kernels of Hilbert type have a general form of

$$T(x) = \frac{1}{x^n} \quad (n=1, 2, \dots) \quad (2)$$

Here, kernel  $T(x)=1/x$  commonly occurs in electrodynamics, theory of linear response, signal processing, theory of analytic functions, and the Hilbert transform. When  $n=2$ ,  $T(x)=1/x^2$  is the kernel used in tomography. Another interesting example is the singular kernels of Abel type

$$T(x) = \frac{1}{x^\beta} \quad (0 < \beta < 1) \quad (3)$$

These kernels can be recognized as the special cases of the singular integral equations of Volterra type of the first kind. The singular kernels of Abel type have applications in the area of holography and interferometry with phase objects (of practical importance in aerodynamics, heat and mass transfer, and plasma diagnostics). They are intimately connected with the Radon transform, for example, in determining the refractive index from the knowledge of a holographic interferogram. The other important example is the singular kernels of delta type

$$T(x) = \delta^{(n)}(x) \quad (n=0, 1, 2, \dots) \quad (4)$$

Here, kernel  $T(x)=\delta(x)$  is of particular importance for interpolation of surfaces and curves (including atomic, molecular and biological potential energy surfaces, engineering surfaces and a variety of image processing and pattern recognition problems involving low-pass filters). Higher-order kernels,  $T(x)=\delta^{(n)}(x)$ , ( $n=1, 2, \dots$ ) are essential for numerically solving partial differential equations and for image processing, noise estimation, etc. However, since these kernels are singular, they cannot be directly digitized in computers. Hence, the singular convolution, (1), is of little numerical merit. To avoid the difficulty of using singular expressions directly in computers, we construct sequences of approximations ( $T_\alpha$ ) to the distribution  $T$

$$\lim_{\alpha \rightarrow \alpha_0} T_\alpha(x) \rightarrow T(x) \quad (5)$$

where  $\alpha_0$  is a generalized limit. Obviously, in the case of  $T(x)=\delta(x)$ , each element in the sequence,  $T_\alpha(x)$ , is a delta sequence kernel. Note that one retains the delta distribution at the limit of a delta sequence kernel. Computationally, the Fourier transform of the delta distribution is unity. Hence, it is a *universal reproducing kernel* for numerical computations and an

*all pass filter* for image and signal processing. Therefore, the delta distribution can be used as a starting point for the construction of either band-limited reproducing kernels or approximate reproducing kernels. By the Heisenberg uncertainty principle, exact reproducing kernels have bad localization in the time (spatial) domain, whereas, approximate reproducing kernels can be localized in both time and frequency representations. Furthermore, with a sufficiently smooth approximation, it is useful to consider a *discrete singular convolution* (DSC)

$$F_z(t) = \sum_k T_z(t - x_k) f(x_k) \quad (6)$$

where  $F_z(t)$  is an approximation to  $F(t)$  and  $\{x_k\}$  is an appropriate set of discrete points on which the DSC, Equation (6), is well defined. Note that, the original test function  $\eta(x)$  has been replaced by  $f(x)$ . The mathematical property or requirement of  $f(x)$  is determined by the approximate kernel  $T_z$ . In general, the convolution is required being Lebesgue integrable. In the rest of this paper, the emphasis is on the singular kernels of delta type, including their approximation, and numerical implementation.

*2.1.1. Singular kernels of delta type.* The delta distribution or the so-called Dirac delta function ( $\delta$ ) is a generalized function which is integrable inside a particular interval but in itself does not need to have a value. Heaviside introduced both the unit step Heaviside function and the Dirac delta function as its derivative and referred to the latter as the unit impulse. Dirac, for the first time, explicitly discussed the properties of  $\delta$  in his classic text on quantum mechanics; for this reason  $\delta$  is often called the Dirac delta function. However, the delta distribution has a history which antedates both Heaviside and Dirac. It appeared in an explicit form as early as 1822, in Fourier's *Théorie Analytique de la Chaleur*. The work of Heaviside, and subsequently of Dirac, in the systematic but informal exploitation of the step and the delta functions, has made the delta distribution familiar to physicists and engineers before Sobolev, Schwartz [30], Korevaar [39] and others put it into a rigorous mathematical form. The Dirac delta function is the most important special case of distributions or generalized functions. There are three parallel descriptions for the theory of distributions. One description of distributions is to characterize them as an equivalence class, or as a generalized limit of various Cauchy sequences (fundamental sequences) and fundamental families as rigorously defined by Korevaar [39]. This approach is particularly convenient for the delta distribution. Another description is to formulate them as continuous linear functionals on the space of test functions as introduced by Schwartz [30]. The vector space of test functions is obtained from a class of test functions with compatible convergence or topology. The other description is based on generalized derivatives of integrable functions. The generalized derivatives are distributions rather than well-behaved functions. The first description is intuitive and convenient for various applications. The second description is particularly elegant and concise. It is also very convenient for higher dimensional applications. The third description is useful for certain practical applications involving derivatives and antiderivatives. These three descriptions are formally equivalent and are commonly used for describing not only for the delta distribution, but also for distributions in general. The use of many delta sequences as probability density estimators was discussed by Walter and Blum [40] and others [41–43].

*Definition 1*

The delta distribution, or the so-called Dirac delta function is given as a continuous linear functional on the space of test functions,  $\mathcal{D}(-\infty, \infty)$ ,

$$\langle \delta, \phi \rangle = \delta(\phi) = \int_{-\infty}^{\infty} \delta \phi = \phi(0) \quad (7)$$

A delta sequence kernel,  $\{\delta_x(x)\}$ , is a sequence of kernel functions on  $(-\infty, \infty)$  which is integrable over every compact domain and their inner product with every test function  $\phi$  converges to the delta distribution

$$\lim_{\alpha \rightarrow \alpha_0} \int_{-\infty}^{\infty} \delta_x \phi = \langle \delta, \phi \rangle \quad (8)$$

where the (real or complex) parameter  $\alpha$  approaches  $\alpha_0$ , which can either be  $\infty$  or a limit value, depending on the situation (such a convention for  $\alpha_0$  is used through out this paper). If  $\alpha_0$  represents a limit value, the corresponding delta sequence kernel is a fundamental family. Depending on the explicit form of  $\delta_x$ , the condition on  $\phi$  can be relaxed. For example, if  $\delta_x$  is given as

$$\delta_x(x) = \begin{cases} \alpha & \text{for } 0 < x < 1/\alpha \\ 0 & \text{otherwise} \end{cases} \quad \alpha = 1, 2, \dots, \quad (9)$$

then Equation (8) makes sense for every  $\phi$  in  $C(-\infty, \infty)$ .

There are many delta sequence kernels arising in the theory of partial differential equations, Fourier transforms and signal analysis, with completely different mathematical properties. It is useful to have a classification of various delta sequence kernels for discussion, application and for new construction. The delta sequence kernels of positive and Dirichlet type have very distinct mathematical properties and can serve as the basis of a good classification scheme. In particular, there is a close relation between the delta sequence kernel of positive type and statistical distribution functions. In fact, every statistical distribution function can be regarded as an element of the delta sequence kernel of positive type. An ordinary element of the delta sequence kernel of Dirichlet type has the well-known feature of 'small wave'. In other words it is readily related to the wavelet scaling function. Moreover, classifying delta sequence kernels according to Schwartz class or non-Schwartz class is also very useful for various applications in physical and engineering sciences. In particular, all physically realizable states, either in the sense of quantum mechanics or classical mechanics, belong to the Schwartz class [44]. Moreover, for the purpose of numerical applications to ill-posed problems, delta sequences of the Schwartz class are applicable to a wide class of functions and distributions. In the following two subsections, the delta sequence kernels of positive type and Dirichlet type are studied.

*2.1.2. Delta sequence kernels of positive type**Definition 2*

Let  $\{\delta_x\}$  be a sequence of kernel functions on  $(-\infty, \infty)$  which are integrable over every bounded interval. We call  $\{\delta_x\}$  a delta sequence kernel of positive type if

1.  $\int_{-a}^a \delta_x \rightarrow 1$  as  $\alpha \rightarrow \alpha_0$  for some finite constant  $a$ .

2. For every constant  $\gamma > 0$ ,  $(\int_{-\infty}^{-\gamma} + \int_{\gamma}^{\infty})\delta_{\alpha} \rightarrow 0$  as  $\alpha \rightarrow \alpha_0$ .
3.  $\delta_{\alpha}(x) \geq 0$  for all  $x$  and  $\alpha$ .

*Example 1*

Delta sequence kernel of impulse functions.

To approximate idealized physical concepts such as the force density of a unit force at the origin  $x=0$ , or a unit impulse at time  $x=0$ , a sequence of functions given by

$$\delta_{\alpha}(x) = \begin{cases} \alpha & \text{for } 0 < x < 1/\alpha, \\ 0 & \text{otherwise} \end{cases} \quad \alpha = 1, 2, \dots \quad (10)$$

is a DSC delta sequence kernel provided  $\alpha \rightarrow \infty$ . This is a commonly used density estimator in science and engineering.

*Example 2*

Gauss' delta sequence kernel.

In the study of the heat equation, Gauss' delta sequence kernel

$$\delta_{\alpha}(x) = \frac{1}{\sqrt{2\pi\alpha}} e^{-x^2/(2\alpha^2)} \quad \text{for } \alpha \rightarrow 0 \quad (11)$$

arises naturally as a distribution solution or so-called weak solution. Gauss' delta sequence kernel has various interesting properties with regard to differentiability, boundedness and Fourier transforms, and it is used to generate the 'Mexican hat' wavelet.

*Example 3*

Lorentz's delta sequence kernel.

Lorentz's delta sequence kernel

$$\delta_{\alpha}(x) = \frac{1}{\pi} \frac{\alpha}{x^2 + \alpha^2} \quad \text{for } \alpha \rightarrow 0 \quad (12)$$

is known for its role in representing the solution of the Laplace equation in the upper half plane. It is commonly seen in integral equations involving Green's function of the kinetic energy operator (in the momentum representation). It is also the expression for the line shape of various spectroscopies when the relaxation is an exponential one in the time domain. A generalized expression can be written as

$$\delta_{\alpha,n}(x) = \frac{1}{\pi} \frac{\alpha^n x^{n-1}}{x^{2n} + \alpha^{2n}} \quad \text{for } \alpha \rightarrow 0 \text{ and } n \geq 1 \quad (13)$$

This includes Equation (12) as a special case.

*Example 4*

Landau's delta sequence kernel.

In the discussion of convergence properties of polynomial approximations, Landau introduced a delta sequence kernel

$$L_n(x) = \frac{(a^2 - x^2)^n}{\int_{-a}^a (a^2 - y^2)^n dy} \quad \text{for } n=0, 1, 2, \dots \text{ and } a > 0 \quad (14)$$

It becomes a delta sequence kernel

$$\delta_n(x) = \begin{cases} L_n(x) & \text{for } |x| \leq a, \\ 0 & \text{otherwise} \end{cases} \quad (15)$$

as  $n \rightarrow \infty$ . This is called Landau's delta sequence kernel. Wavelets generated from Landau's delta sequence kernel can be very useful for a sufficiently large  $n$ .

*Example 5*

Poisson's delta sequence kernel family.

The function given by the summation of an infinite series

$$\begin{aligned} P_\alpha(x) &= \frac{1}{\pi} \left[ \frac{1}{2} + \alpha \cos(x) + \alpha^2 \cos(2x) + \dots \right] \\ &= \frac{1 - \alpha^2}{2\pi[1 - 2\alpha \cos(x) + \alpha^2]} \end{aligned}$$

where  $0 \leq \alpha < 1$  and  $(-\infty < x < \infty)$ , is called the Poisson kernel, which plays an important role in Poisson's integral formulae. Poisson's delta sequence kernel family is given by

$$\delta_\alpha(x) = \begin{cases} P_\alpha(x) & \text{for } |x| \leq \pi, \\ 0 & \text{otherwise} \end{cases} \quad (16)$$

as  $\alpha \rightarrow 1$ . Poisson's delta sequence kernel family has a connection with the solution of the Laplace equation in a unit disc (i.e. the Dirichlet problem for a unit disc).

*Example 6*

Fejér's delta sequence kernel.

The partial sum of the discrete Fourier series

$$\begin{aligned} D_k(x) &= \frac{1}{\pi} \left[ \frac{1}{2} + \cos(x) + \cos(2x) + \dots + \cos(kx) \right] \\ &= \frac{\sin[(k + \frac{1}{2})x]}{2\pi \sin(\frac{1}{2}x)}, \quad k=0, 1, 2, \dots \end{aligned} \quad (17)$$

is called a Dirichlet kernel. To improve convergence for proving a trigonometric approximation theorem, Fejér introduced the following arithmetic mean:

$$\begin{aligned} F_k(x) &= \frac{1}{k} [D_0(x) + D_1(x) + \cdots + D_{k-1}(x)] \\ &= \frac{\sin^2(\frac{1}{2}kx)}{2\pi k \sin^2(\frac{1}{2}x)} \quad -\infty < x < \infty \end{aligned} \quad (18)$$

Then Fejér's delta sequence kernel is given by

$$\delta_\alpha(x) = \begin{cases} F_\alpha(x) & \text{for } |x| \leq \pi \\ 0 & \text{otherwise} \end{cases} \quad \text{for } \alpha = 0, 1, 2, \dots \quad (19)$$

as  $\alpha \rightarrow \infty$ . Fejér's delta sequence kernel has an important application in the theory of reproducing kernels. It also describes the intensity pattern of light from a regular series of pinholes in optical physics.

#### Example 7

Generalized Fejér's delta sequence kernel.

It is noted that Fejér's method of generating the delta sequence kernel is very general. Essentially, a family of arithmetic means of delta sequence kernels are still delta sequence kernels. The resulting delta sequence kernel can be called a delta sequence kernel of Fejér type. For instance, in a similar treatment using Dirichlet's continuous delta sequence kernels (see next subsection), one obtains the following Fejér's continuous delta sequence kernel:

$$\delta_\alpha(x) = \frac{2 \sin^2(\alpha x)}{\pi \alpha x^2} \quad \forall x \in R \quad (20)$$

Obviously, this is well defined on the real line. This expression is related to the intensity of light diffracted by a uniform slit.

#### Example 8

Delta sequence kernels generated by dilation.

Let  $\rho \in L^1(R)$  be a non-negative function with  $\int \rho(x) dx = 1$ , dilation of  $\rho$  given by

$$\rho_\alpha(x) = \frac{1}{\alpha} \rho\left(\frac{x}{\alpha}\right) \quad (\alpha > 0) \quad (21)$$

leads to a delta sequence kernel,  $\rho_\alpha \rightarrow \delta$ , as  $\alpha \rightarrow 0$ .

Physically,  $\rho$  can be regarded as a statistical distribution function. This is a general procedure and *Examples 2* and *3* fit into this structure. *Examples 1* and *6* can be expressed in this form by appropriate modifications (by replacing  $\alpha$  with  $\beta = 1/\alpha$ , and then letting  $\beta \rightarrow 0$ ).

### 2.1.3. Delta sequence kernels of Dirichlet type

#### Definition 3

Let  $\{\delta_\alpha\}$  be a sequence of functions on  $(-\infty, \infty)$  which are integrable over every bounded interval. We call  $\{\delta_\alpha\}$  a delta sequence kernel of Dirichlet type if

1.  $\int_{-a}^a \delta_\alpha \rightarrow 1$  as  $\alpha \rightarrow \alpha_0$  for some finite constant  $a$ .
2. For every constant  $\gamma > 0$ ;  $(\int_{-\infty}^{-\gamma} + \int_{\gamma}^{\infty}) \delta_\alpha \rightarrow 0$  as  $\alpha \rightarrow \alpha_0$ .
3. There are positive constants  $C_1$  and  $C_2$  such that

$$|\delta_\alpha(x)| \leq \frac{C_1}{|x|} + C_2$$

for all  $x$  and  $\alpha$ .

#### Example 1

Dirichlet delta sequence kernel.

The most important example of a delta sequence kernel of Dirichlet type is the Dirichlet delta sequence kernel

$$\delta_\alpha(x) = \begin{cases} D_\alpha(x) & \text{for } |x| \leq \pi \\ 0 & \text{otherwise} \end{cases} \quad \text{for } \alpha = 0, 1, 2, \dots \quad (22)$$

where  $D_\alpha$  is the Dirichlet kernel given by Equation (17). Dirichlet's delta sequence kernel plays an important role in approximation theory and is the key element in trigonometric polynomial approximations. In fact, it is an exact reproducing kernel for bandlimited, periodic,  $L^2$  functions. Physically, it describes the diffraction of light passing through a regular series of pinholes in which the  $k$ th pinhole's contribution is proportional to  $e^{ik}$ .

#### Example 2

Modified Dirichlet delta sequence kernel.

Sometimes there is some advantage in taking the last term in  $D_\alpha$  with a factor of  $\frac{1}{2}$ :

$$\begin{aligned} D_\alpha^*(x) &= D_\alpha - \frac{1}{2\pi} \cos(\alpha x) \\ &= \frac{\sin(\alpha x)}{2\pi \tan(\frac{1}{2}x)}, \quad \alpha = 0, 1, 2, \dots \end{aligned} \quad (23)$$

This is the so-called modified Dirichlet kernel. The difference  $D_\alpha - D_\alpha^*$  tends uniformly to zero on  $(-\pi, \pi)$  as  $\alpha \rightarrow \infty$ . They are equivalent with respect to convergence.

The expression given by

$$\delta_\alpha(x) = \begin{cases} D_\alpha^*(x) & \text{for } |x| \leq \pi \\ 0 & \text{otherwise} \end{cases} \quad \text{for } \alpha = 0, 1, 2, \dots \quad (24)$$

is a delta sequence kernel of Dirichlet type as  $\alpha \rightarrow \infty$ .

*Example 3*

Lagrange delta sequence kernel.

The Lagrange interpolation formula

$$L_{M,k}(x) = \prod_{i=k-M, i \neq k}^{i=k+M} \frac{x - x_i}{x_k - x_i}, \quad (M \geq 1) \tag{25}$$

is defined on an interval  $(a, b)$  with a set of  $2M + 1$  ordered discrete points,

$$\{x_i\}_{i=k-M}^{k+M}: x_{k-M} = a < x_{k-M+1} < \dots < x_k < \dots < x_{k+M} = b \tag{26}$$

It converges to the delta distribution as

$$a \rightarrow -\infty, \quad b \rightarrow \infty \quad \text{and} \quad \sup_{\forall x_i, x_j \in (a, b)} |x_i - x_j| \rightarrow 0 \tag{27}$$

Obviously, these limits imply  $M \rightarrow \infty$ . Since the delta distribution has only a point support, the Lagrange interpolation formula is a delta sequence

$$\delta_{M,k}(x) = \begin{cases} L_{M,k}(x) & \text{for } a \leq x \leq b \\ 0 & \text{otherwise} \end{cases} \quad \text{for } M = 1, 2, \dots \tag{28}$$

as  $M \rightarrow \infty$  (to qualify as a delta sequence of Dirichlet type,  $M \geq 2$  is required in Equation (28)).

*Example 4*

Interpolative delta sequence kernel.

Let  $\{\delta_n\}$  be a sequence of functions converging to the delta distribution and let  $\{x_i\}_0^n$  be  $n + 1$  zeroes of a Jacobi polynomial in  $(a, b)$ .

$$\Delta_n(x, y) = \frac{\prod_{i=0}^n (x - x_i)}{(x - y) \prod_{i=0}^n (y - x_i)} \sum_{i=0}^n \delta_n(y - x_i), \quad x, y \in (a, b) \tag{29}$$

is a delta sequence kernel as  $n \rightarrow \infty$ . This follows from the fact that  $\int \Delta_n(x, y) f(y) dy$  are approximations to the Lagrange interpolation formula.

*Example 5*

de la Vallée Poussin delta sequence kernel.

The de la Vallée Poussin kernel is given by

$$\begin{aligned} P_{n,p}(x) &= \frac{1}{p+1} \sum_{k=n-p}^n D_k(x) \\ &= \frac{1}{2\pi} + \frac{1}{\pi} \sum_{k=1}^{n-p} \cos kx + \frac{1}{\pi} \sum_{k=1}^p \left[ 1 - \frac{k}{p+1} \right] \cos[(n-p+k)x] \\ &= \frac{\sin[(2n+1-p)x/2] \sin[(p+1)x/2]}{2\pi(p+1) \sin^2(x/2)}, \quad p=0, \dots, n; \quad n=0, 1, \dots \end{aligned} \tag{30}$$

where  $D_k(x)$  are the Dirichlet kernels given by Equation (17). It is interesting to note that the de la Vallée Poussin kernel reduces to the positively defined Ferér's kernel  $F_{n+1}(x)$  when  $p=n$ . The de la Vallée Poussin delta sequence kernel is given by

$$\delta_{n,p}(x) = \begin{cases} P_{n,p}(x) & \text{for } |x| \leq \pi \\ 0 & \text{otherwise} \end{cases} \quad \text{for } p=0, \dots, n; \quad n=0, 1, \dots \quad (31)$$

as  $n, p \rightarrow \infty$ . The de la Vallée Poussin delta sequence kernel is of Dirichlet type when  $p < n$ .

A simplified de la Vallée Poussin kernel given by

$$\delta_\alpha(x) = \frac{1}{\pi\alpha} \frac{\cos(\alpha x) - \cos(2\alpha x)}{x^2} \quad (32)$$

is found to be very useful numerically [26].

#### Example 6

DSC kernels constructed by orthogonal basis expansions.

Let  $\{\psi_i\}$  be a complete orthonormal  $L^2(a, b)$  basis. Then

$$\delta_n(x, y) = \sum_{i=0}^n \psi_i(x) \psi_i(y), \quad x, y \in (a, b) \quad (33)$$

are DSC delta sequence kernels. In the case of trigonometric functions, we again obtain the Dirichlet kernels given in the *Examples 1* and *3*. The Hermite function expansion is given by

$$\delta_n(x) = \exp(-x^2) \sum_{k=0}^n \left(\frac{-1}{4}\right)^k \frac{1}{\sqrt{\pi k!}} H_{2k}(x), \quad \forall x \in \mathbb{R} \quad (34)$$

where  $H_{2k}(x)$  is the usual Hermite polynomial. Note that the Hermite kernel in Equation (34) has a different form from Equation (33). This is because it is evaluated at  $x=0$  in the series expansion.

#### Example 7

Shannon's delta sequence kernel.

Shannon's delta sequence kernel (or Dirichlet's continuous delta sequence kernel) is given by the following (inverse) Fourier transform of the characteristic function,  $\chi_{[-\alpha/2\pi, \alpha/2\pi]}$ ,

$$\begin{aligned} \delta_\alpha(x) &= \int_{-\infty}^{\infty} \chi_{[-\frac{\alpha}{2\pi}, \frac{\alpha}{2\pi}]} e^{-i2\pi\zeta x} d\zeta \\ &= \frac{\sin(\alpha x)}{\pi x} \end{aligned} \quad (35)$$

Alternatively, Shannon's delta sequence kernel can be given as an integration

$$\delta_\alpha(x) = \frac{1}{\pi} \int_0^\alpha \cos(xy) \, dy \quad (36)$$

or as the limit of a continuous product

$$\delta_\alpha(x) = \lim_{N \rightarrow \infty} \frac{\alpha}{\pi} \prod_{k=1}^N \cos\left(\frac{\alpha}{2^k} x\right) = \lim_{N \rightarrow \infty} \frac{1}{2^N \pi} \frac{\sin(\alpha x)}{\sin[(\alpha/2^N)x]} \quad (37)$$

Numerically, Shannon's delta sequence kernel is one of the most important cases, because of its property of being an element of the Paley–Wiener reproducing kernel Hilbert space  $B_{1/2}^2$

$$f(x) = \int_{-\infty}^{\infty} f(y) \frac{\sin[\pi(x-y)]}{\pi(x-y)} \, dy, \quad \forall f \in B_{1/2}^2 \quad (38)$$

where  $\forall f \in B_{1/2}^2$  indicates that, in its Fourier representation, the  $L^2$  function  $f$  vanishes outside the interval  $[-\frac{1}{2}, \frac{1}{2}]$ . The Paley–Wiener reproducing kernel Hilbert space  $B_{1/2}^2$  is a subspace of the Hilbert space  $L^2(R)$ . It is noted that the reproducing kernel Hilbert space is a special class of Hilbert space. For instance, the space  $L^2(R)$  is not a reproducing kernel Hilbert space.

#### Example 8

Generalized Lagrange delta sequence kernel.

Shannon's delta sequence kernel can be derived from the generalized Lagrange interpolation formula

$$S_k(x) = \frac{G(x)}{G'(x_k)(x - x_k)} \quad (39)$$

where  $G(x)$  is an entire function given by

$$G(x) = (x - x_0) \prod_{k=1}^{\infty} \left(1 - \frac{x}{x_k}\right) \left(1 - \frac{x}{x_{-k}}\right) \quad (40)$$

and  $G'$  denotes the derivative of  $G$ . For a function bandlimited to  $B$ , the generalized Lagrange interpolation formula  $S_k(x)$  of Equation (39) can provide an exact result

$$f(x) = \sum_{k \in Z} f(y_k) S_k(x) \quad (41)$$

whenever the set of non-uniform sampling points satisfy

$$\sup_{k \in Z} \left| x_k - \frac{k\pi}{B} \right| < \frac{\pi}{4B} \quad (42)$$

where the symbol  $Z$  denotes the set of all integers. This is called the Paley and Wiener sampling theorem in the literature.

If  $\{x_k\}_{k \in \mathbb{Z}}$  are limited to a set of points on a uniform infinite grid ( $x_k = k\Delta = -x_{-k}$ ), Equation (40) can be simplified

$$G(x) = x \prod_{k=-\infty, k \neq 0}^{\infty} \left(1 - \frac{x}{k\Delta}\right) \tag{43}$$

$$= x \prod_{k=1}^{\infty} \left(1 - \frac{x^2}{k^2\Delta^2}\right) \tag{44}$$

$$= \Delta \frac{\sin[(\pi/\Delta)x]}{\pi} \tag{45}$$

Since  $G'(x_k)$  reduces to

$$G'(x_k) = (-1)^k \tag{46}$$

on a uniform grid, Equation (39) gives rise to

$$S_k(x) = \frac{G(x)}{G'(x_k)(x - x_k)} = \frac{(-1)^k \sin[(\pi/\Delta)x]}{(\pi/\Delta)(x - k\Delta)} \tag{47}$$

$$= \frac{\sin[(\pi/\Delta)(x - x_k)]}{(\pi/\Delta)(x - x_k)} \tag{48}$$

Obviously,  $\sin[\pi/\Delta(x - x_k)]/[\pi/\Delta(x - x_k)]$  is an approximation to the delta distribution

$$\lim_{\Delta \rightarrow 0} \frac{\sin[(\pi/\Delta)(x - x_k)]}{(\pi/\Delta)(x - x_k)} \rightarrow \delta(x - x_k) \tag{49}$$

In fact, the generalized Lagrange interpolation formula directly gives rise to the delta distribution under an appropriate limit

$$\lim_{\max \Delta x \rightarrow 0} S_k(x) = \lim_{\max \Delta x \rightarrow 0} \frac{G(x)}{G'(x_k)(x - x_k)} \rightarrow \delta(x - x_k) \tag{50}$$

where  $\max \Delta x$  is the largest  $\Delta x$  on the grid.

In the following, the delta sequence kernel is also referred to as the delta kernel. A comparison of two types of delta kernels is given in Figure 1.

### 2.2. Wavelet and time-frequency analyses

This subsection is devoted to wavelet property of the DSC kernels. A regularization procedure is introduced to enhance the time-frequency localization of the DSC kernels.

*2.2.1. Connection to wavelets.* The DSC approximation to the delta distribution is closely related to the theory of wavelets and frames. Mathematically, wavelets are functions generated from a single function by applying dilation and translation. They form building blocks for some spaces, such as  $L^2(R)$ , whether as a frame or as an orthonormal basis. Such building blocks are computationally important when they have certain regularity and localization in both time and frequency domains. Physically, the wavelet transform is a mathematical technique

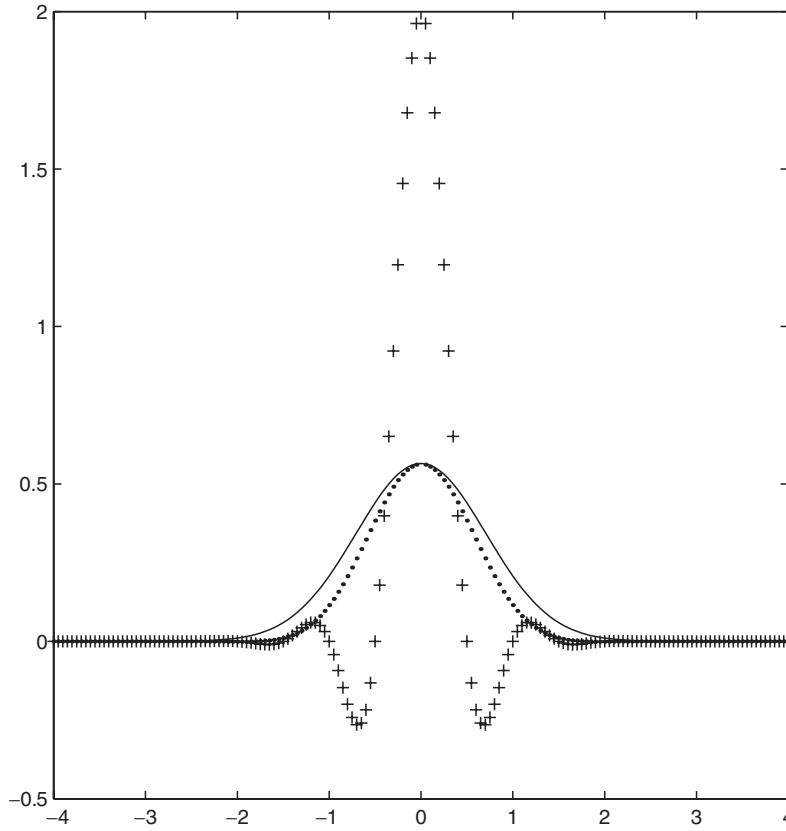


Figure 1. A comparison of delta sequence kernels of the positive type and Dirichlet type. The solid line:  $1/\sqrt{\pi}e^{-x^2}$ ; Dots:  $1/\pi(\sin(x)/x)e^{-x^2}$ ; Crosses:  $1/\pi(\sin(2\pi x)/x)e^{-x^2}$ .

that can be used to split a signal into different frequency bands or components so that each component can be studied with a resolution matched to its scale, thus providing excellent frequency and spatial resolution, and achieving computational efficiency.

Shannon’s wavelet is one of the most important examples and its scaling function is Shannon’s delta kernel,

$$\phi(x) = \frac{\sin(\pi x)}{\pi x} \tag{51}$$

As a delta kernel, it is normalized

$$\hat{\phi}(0) = \int \phi(x) dx = 1 \tag{52}$$

and its Fourier transform is given by the characteristic function  $\hat{\phi}(\omega) = \chi_{[-1/2, 1/2]}$ . It is easy to see that

$$\sum_{n=-\infty}^{\infty} \hat{\phi}(\omega + n) = 1 \tag{53}$$

and

$$\sum_{n=-\infty}^{\infty} |\hat{\phi}(\omega + n)|^2 = 1 \quad (54)$$

Equation (54) is a consequence of orthonormality. In fact, the sequence of functions  $\{\phi(x - n)\}_{n=-\infty}^{\infty}$  are orthonormal.

Shannon's mother wavelet can be constructed from Shannon's delta kernel (Shannon's wavelet scaling function)

$$\psi(x) = \frac{\sin(2\pi x) - \sin(\pi x)}{\pi x} \quad (55)$$

with its Fourier expression

$$\hat{\psi}(\omega) = \chi_{[-1,1]}(\omega) - \chi_{[-1/2,1/2]}(\omega) \quad (56)$$

This is recognized as the ideal band pass filter and it satisfies the orthonormality conditions

$$\sum_{n=-\infty}^{\infty} \hat{\psi}(\omega + n) = 1 \quad (57)$$

and

$$\sum_{n=-\infty}^{\infty} |\hat{\psi}(\omega + n)|^2 = 1 \quad (58)$$

Technically, it can be shown that a system of orthogonal wavelets are generated from a single function, the 'mother' wavelet  $\psi$ , by standard operations of translation and dilation

$$\psi_{mn}(x) = 2^{-m/2} \psi\left(\frac{x}{2^m} - n\right), \quad m, n \in Z \quad (59)$$

A family of Shannon's wavelet scaling functions  $\{\psi_{mn}(x)\}_{n,m \in Z}$  span a series of orthogonal wavelet subspaces  $\{W_m\}_{m \in Z}$  satisfying

$$\bigoplus_{m \in Z} W_m = L^2(R) \quad (60)$$

Alternatively, a family of Shannon's wavelet scaling functions  $\{\phi_{mn}(x)\}_{n,m \in Z}$  are constructed from a single Shannon's delta kernel

$$\phi_{mn}(x) = 2^{-m/2} \phi\left(\frac{x}{2^m} - n\right), \quad m, n \in Z \quad (61)$$

They span a series of nested wavelet subspaces  $\{V_m\}_{m \in Z}$ . Each corresponds to a different resolution

$$\cdots \subset V_{-1} \subset V_0 \subset V_1 \subset \cdots \subset L^2(R) \quad (62)$$

This nested structure provides the conceptual basis for the wavelet multiresolution analysis.

From the point of view of signal processing, Shannon's delta kernel  $\phi_x$  corresponds to a family of *ideal low pass filters*, each with a different bandwidth

$$\phi_x(x) = \frac{\sin(\alpha x)}{\pi x} \quad (63)$$

Their corresponding wavelet expressions

$$\psi_z(x) = \frac{\sin(2\alpha x) - \sin(\alpha x)}{\pi x} \quad (64)$$

are band pass filters. However, Shannon's wavelet system is seldom used in real applications because it requires infinitely many data points. In the next subsection, we discuss a practical approach for generating powerful filters from Shannon's delta kernel.

Two wavelet generators were introduced [28] to create wavelets from the DSC kernels systematically. For example, Gauss-kernel-generated wavelets are given by

$$\psi_n(x) = G^n \frac{1}{\sqrt{\pi}} e^{-x^2} = \frac{1}{\sqrt{\pi}} \frac{(-1)^n}{2} H_{n+1}(x) e^{-x^2} \quad n=0, 1, 2, \dots \quad (65)$$

where  $H_{n+1}$  is the  $(n+1)$ th order Hermite polynomial and  $G^n$  is a wavelet generator

$$G^n = x \frac{\partial^n}{\partial x^n} + n \frac{\partial^{n-1}}{\partial x^{n-1}}, \quad n=0, 1, 2, \dots \quad (66)$$

Equation (65) gives rise to a few important cases in image processing, e.g. the Canny operator is given by  $n=0$  and the celebrated Mexican hat wavelet is given by  $n=1$ . These wavelets are useful in digital image edge detection.

**2.2.2. Regularization.** Both  $\phi(x)$  and its associated wavelet play a crucial role in information theory and the theory of signal processing. However their usefulness is limited by the fact that  $\phi(x)$  and  $\psi(x)$  are infinite impulse response (IIR) filters and their Fourier transforms  $\hat{\phi}(\omega)$  and  $\hat{\psi}(\omega)$  are not differentiable. From the computational point of view,  $\phi(x)$  and  $\psi(x)$  do not have finite moments in the co-ordinate space; in other words, they are de-localized. This non-local feature in the co-ordinate is related to its bandlimited character in the Fourier representation by the Heisenberg uncertainty principle.

According to the theory of distributions, the smoothness, regularity and localization of a temper distribution can be improved by a function of the Schwartz class. We apply this principle to regularize singular convolution kernels

$$\Phi_\sigma(x) = R_\sigma(x) \phi(x), \quad (\sigma > 0) \quad (67)$$

where  $R_\sigma$  is a *regularizer* which has properties

$$\lim_{\sigma \rightarrow \infty} R_\sigma(x) = 1 \quad (68)$$

and

$$R_\sigma(0) = 1 \quad (69)$$

Here Equation (68) is a general condition that a regularizer must satisfy, while Equation (69) is specifically for a *delta regularizer*, which is used in regularizing a delta kernel. Various delta regularizers can be used for numerical computations. A good example is the Gaussian

$$R_\sigma(x) = \exp \left[ -\frac{x^2}{2\sigma^2} \right] \quad (70)$$

Gaussian regularizer is a Schwartz class function and has excellent numerical performance. However, we noted that in certain eigenvalue problems, no regularization is required if the potential is smooth and bounded from below (e.g. the harmonic oscillator potential  $\frac{1}{2}x^2$ ).

Immediate benefit from the regularized Shannon’s kernel function Equation (67) is that its Fourier transform is infinitely differentiable because the Gaussian is an element of Schwartz class functions. Qualitatively, all kernels of Dirichlet type oscillate in the co-ordinate representation. Shannon’s kernel has a long tail which is proportional to  $1/x$ , whereas, the regularized kernels decay exponentially fast, especially when the  $\sigma$  is very small. In the Fourier representation, Shannon’s kernel is an ideal low pass filter, which is discontinuous at  $\omega = \pm \frac{1}{2}$ . In contrast, all regularized Shannon’s kernels have an ‘optimal’ shape in their frequency responses. Of course, they all reduce to Shannon’s low pass filter at the limit

$$\lim_{\sigma \rightarrow \infty} \Phi_{\sigma}(x) = \lim_{\sigma \rightarrow \infty} \frac{\sin(\pi x)}{\pi x} e^{-x^2/(2\sigma^2)} = \frac{\sin(\pi x)}{\pi x} \tag{71}$$

Quantitatively, one can examine the normalization of  $\Phi_{\sigma}(x)$

$$\begin{aligned} \hat{\Phi}_{\sigma}(0) &= \int \Phi_{\sigma}(x) dx \\ &= \sqrt{2\pi}\sigma \sum_{k=0}^{\infty} \frac{(-1)^k}{k!(2k+1)} \left(\frac{\pi\sigma}{\sqrt{2}}\right)^{2k} \end{aligned} \tag{72}$$

By means of the error function,  $\text{erf}(z) = 2/\sqrt{\pi} \int_0^z e^{-t^2} dt$ , Equation (72) can be rewritten as

$$\begin{aligned} \hat{\Phi}_{\sigma}(0) &= \text{erf}\left(\frac{\pi\sigma}{\sqrt{2}}\right) \\ &= 1 - \sqrt{\frac{2}{\pi}} \frac{1}{\sigma} e^{-\sigma^2\pi^2/2} \int_0^{\infty} e^{[-t^2/(2\sigma^2)] - \pi t} dt \\ &= 1 - \text{erfc}\left(\frac{\pi\sigma}{\sqrt{2}}\right) \end{aligned} \tag{73}$$

where  $\text{erfc}(z)$  is the complementary error function. Note that for a given  $\sigma > 0$ ,  $\text{erfc}(\pi\sigma/\sqrt{2})$  is positive definite. Thus,  $\hat{\Phi}_{\sigma}(0)$  is always less than unity except at the limit of  $\sigma \rightarrow \infty$ .

In fact,  $\Phi_{\sigma}(x)$  does not really satisfy the requirement, as given by Equation (52), for a wavelet scaling function. However, when we choose  $\sigma \gg \sqrt{2}/\pi$ , which is the case in many practical applications, the residue term,  $\text{erfc}(\pi\sigma/\sqrt{2})$ , approaches zero very quickly. As a result,  $\hat{\Phi}_{\sigma}(0)$  is extremely close to unity. Therefore, we call the regularized Shannon’s delta kernel  $\Phi_{\sigma}$  a quasi-wavelet scaling function.

### 2.3. Discretization

For the purpose of digital computations, it is necessary to discretize various delta kernels. To this end, we should examine a *sampling basis* given by Shannon’s delta kernel

$$S_k(x) = \frac{\sin[\pi(x - x_k)]}{\pi(x - x_k)}, \quad \forall k \in Z \tag{74}$$

This sampling basis is an element of the Paley–Wiener reproducing kernel Hilbert space. Hence, it provides a *discrete representation* of every (continuous) function in  $B_{1/2}^2$ , that is

$$f(x) = \sum_{k \in Z} f(x_k) S_k(x), \quad \forall f \in B_{1/2}^2 \quad (75)$$

This is recognized as Shannon's sampling theorem and it means that one can recover a continuous bandlimited  $L^2$  function from a set of discrete values. Equation (75) is particularly important to information theory and the theory of sampling because it satisfies the interpolation condition

$$S_n(x_m) = \delta_{n,m} \quad (76)$$

where  $\delta_{n,m}$  is the Kronecker delta function. Note that Shannon's delta kernel is obviously interpolative on  $Z$ . Computationally, being interpolative is desirable for numerical accuracy and simplicity.

On a grid of arbitrary spacing  $\Delta$ , Shannon's sampling theorem can be modified as

$$f(x) = \sum_{k \in Z} f(x_k) \frac{\sin[(\pi/\Delta)(x - x_k)]}{(\pi/\Delta)(x - x_k)}, \quad \forall f \in B_{1/2\Delta}^2 \quad (77)$$

This suggests that we can discretize the regularized Shannon's delta kernel as

$$\Phi_{\sigma,\Delta}(x - x_k) = \frac{\sin[(\pi/\Delta)(x - x_k)]}{(\pi/\Delta)(x - x_k)} e^{-(x-x_k)^2/(2\sigma^2)} \quad (78)$$

It is noted that if  $\Delta$  is chosen as the spatial mesh size (this is, in general, not required in signal and image processing),  $\Phi_{\sigma,\Delta}(x - x_k)$  retains the interpolation property,

$$\Phi_{\sigma,\Delta}(x_m - x_k) = \delta_{m,k} \quad (79)$$

This is of particular merit for numerical computations.

In practical applications, Equation (77) can never be realized because it requires infinitely many sampling points. Therefore, it is both necessary and convenient to truncate the infinite summation in Equation (77) to a finite  $(2M + 1)$  summation

$$f(x) \approx \sum_{k=-M}^M \delta_{\sigma,\Delta}(x - x_k) f(x_k) \quad (80)$$

where  $\delta_{\sigma,\Delta}(x - x_k)$  is a collective symbol for delta kernels of Dirichlet type. The truncation error is dramatically reduced by the introduction of a delta regularizer. A rigorous proof of this has been given by Qian and Wei [45].

The discretization of the Dirichlet kernel is not as straightforward as that of Shannon's kernel. However, it can be carried out according to the following Dirichlet sampling theorem:

*Theorem*

If an  $L^2$  function  $f(x)$  satisfies the Dirichlet boundary condition and is periodic in  $T$  and bandlimited to the highest (radial) frequency  $2\pi L/T$ , it can be exactly reconstructed from a

finite set of  $2L + 1$  discrete sampling points

$$f(x) = \sum_{k=-L}^L f(x_k) \frac{\sin[(\pi/\Delta)(x - x_k)]}{(2L + 1) \sin[(\pi/\Delta)(x - x_k)/(2L + 1)]} \quad (81)$$

where  $\Delta = T/(2L + 1)$  is the sampling interval and  $x_k = k\Delta$  are the sampling points.

Note that the kernel in Equation (81) differs from that in Equation (17). This follows from a change in the variable  $x \rightarrow (\pi/\Delta y)(2/(2L + 1))y$ , and  $\int dx \rightarrow \sum (\pi/\Delta y)(2/(2L + 1))\Delta y$ . The Dirichlet kernel is a *reproducing kernel* for bandlimited  $L^2$  periodic functions. Therefore, Equation (81) should be the most efficient kernel for numerical computations under the aforementioned conditions. However, to facilitate the Dirichlet kernel in an unbounded computational domain, we use the following regularized discrete expression for the Dirichlet kernel:

$$\frac{\sin[(l + \frac{1}{2})(x - x')]}{2\pi \sin[\frac{1}{2}(x - x')]} \rightarrow \frac{\sin[(\pi/\Delta)(x - x_k)]}{(2L + 1) \sin[(\pi/\Delta)(x - x_k)/(2L + 1)]} \exp\left[-\frac{(x - x_k)^2}{2\sigma^2}\right] \quad (82)$$

Like the regularized Shannon's kernel filter, the present regularized Dirichlet kernel filter has the feature of rapid decay. In comparison to Shannon's kernel, the Dirichlet kernel has one more parameter  $L$  which can be optimized to achieve better results in computations. Usually, we set a sufficiently large  $L$  for various numerical applications. A regularized discrete expression for the modified Dirichlet kernel is

$$\frac{\sin[(l + \frac{1}{2})(x - x')]}{2\pi \tan[\frac{1}{2}(x - x')]} \rightarrow \frac{\sin[(\pi/\Delta)(x - x_k)]}{(2L + 1) \tan[(\pi/\Delta)(x - x_k)/(2L + 1)]} \exp\left[-\frac{(x - x_k)^2}{2\sigma^2}\right] \quad (83)$$

Obviously, the regularized Dirichlet kernel reduces to the regularized Shannon's delta kernel when  $L$  is sufficiently large

$$\begin{aligned} & \lim_{L \rightarrow \infty} \frac{\sin[(\pi/\Delta)(x - x_k)]}{(2L + 1) \sin[(\pi/\Delta)(x - x_k)/(2L + 1)]} \exp\left[-\frac{(x - x_k)^2}{2\sigma^2}\right] \\ &= \lim_{L \rightarrow \infty} \frac{\sin[(\pi/\Delta)(x - x_k)]}{(2L + 1) \tan[(\pi/\Delta)(x - x_k)/(2L + 1)]} \exp\left[-\frac{(x - x_k)^2}{2\sigma^2}\right] \\ &= \frac{\sin[(\pi/\Delta)(x - x_k)]}{(\pi/\Delta)(x - x_k)} \exp\left[-\frac{(x - x_k)^2}{2\sigma^2}\right] \end{aligned} \quad (84)$$

The discretization of the de la Vallée Poussin kernel is given by

$$\begin{aligned} & \frac{1}{\pi\alpha} \frac{\cos[\alpha(x - x')] - \cos[2\alpha(x - x')]}{(x - x')^2} \\ & \rightarrow \frac{2}{3} \frac{\cos[(\pi/\bar{\Delta})(x - x_k)] - \cos[2(\pi/\bar{\Delta})(x - x_k)]}{[(\pi/\bar{\Delta})(x - x_k)]^2} \exp\left[-\frac{(x - x_k)^2}{2\sigma^2}\right] \end{aligned} \quad (85)$$

where  $\bar{\Delta} = \frac{3}{2}\Delta$ . Since  $\pi/\Delta$  is proportional to the highest frequency which can be reached in the Fourier representation, the  $\Delta$  should be very small for a given problem involving very oscillatory functions or very high frequency components.

It is noted that by definition, the Lagrange interpolation formula

$$L_{M,k}(x) = \prod_{i=k-M, i \neq k}^{k+M} \frac{x - x_i}{x_k - x_i} \quad (86)$$

is already discretized. However, its regularized forms

$$\delta_{\sigma}(x - x_k) = \left[ \prod_{i=k-M, i \neq k}^{k+M} \frac{x - x_i}{x_k - x_i} \right] \exp \left[ -\frac{(x - x_k)^2}{2\sigma^2} \right] \quad (87)$$

are very good low pass filters. Unlike the generalized Lagrange interpolation formula, both expressions (86) and (87) are compactly supported kernels. As low pass filters, they require only a finite number of signals and their Fourier transforms have smoothed shoulders as those of regularized Shannon's delta kernels.

#### 2.4. Approximation of derivatives

For the solution of differential equations, one needs to approximate the differential operators. The approximation to derivatives can be constructed by using the DSC kernels of delta type. To start with, we consider a one-dimensional,  $n=0$  order DSC kernel of delta type  $\delta_{\sigma,\Delta}^{(0)}(x-x_k)$ . Approximation to higher order derivatives is given by

$$\delta_{\sigma,\Delta}^{(n)}(x - x_k), \quad (n = 1, 2, \dots) \quad (88)$$

Here  $\delta_{\sigma,\Delta}^{(0)}(x-x_k) = \delta_{\sigma,\Delta}(x-x_k)$  is the DSC delta kernel described in Equation (80). The higher order differentiation matrix elements,  $\delta_{\sigma,\Delta}^{(n)}(x_m - x_k)$ , are obtained by differentiations

$$\delta_{\sigma,\Delta}^{(n)}(x_m - x_k) = \left[ \left( \frac{d}{dx} \right)^n \delta_{\sigma,\Delta}(x - x_k) \right]_{x=x_m} \quad (89)$$

From the point of view of signal processing, these derivatives can be regarded as high pass filters. In fact, the filters corresponding to the derivatives of Shannon's kernel decay slowly as  $x$  increases, whereas, the localization of the regularized DSC filters is controllable because DSC filters are functions of the Schwartz class. In the Fourier representation, the derivatives of Shannon's kernel are discontinuous at certain points. In contrast, all the derivatives of regularized DSC kernels are continuous and can be made very close to those of Shannon's, if desired.

The differentiation in Equation (89) can be *analytically* carried out for a given  $\delta_{\sigma,\Delta}(x-x_k)$ . For example, if  $\delta_{\sigma,\Delta}(x-x_k) = \sin[(\pi/\Delta)(x-x_k)]/[(\pi/\Delta)(x-x_k)]e^{-(x-x_k)^2/(2\sigma^2)}$ , we have for  $x \neq x_k$  the first two terms:

$$\begin{aligned} \delta_{\sigma,\Delta}^{(1)}(x - x_k) &= \frac{\cos [(\pi/\Delta)(x - x_k)]}{x - x_k} \exp \left( -\frac{(x - x_k)^2}{2\sigma^2} \right) \\ &\quad - \frac{\sin [(\pi/\Delta)(x - x_k)]}{(\pi/\Delta)(x - x_k)^2} \exp \left( -\frac{(x - x_k)^2}{2\sigma^2} \right) \\ &\quad - \frac{\sin [(\pi/\Delta)(x - x_k)]}{(\pi/\Delta)\sigma^2} \exp \left( -\frac{(x - x_k)^2}{2\sigma^2} \right) \end{aligned} \quad (90)$$

and

$$\begin{aligned}
\delta_{\sigma,\Delta}^{(2)}(x-x_k) = & -\frac{(\pi/\Delta)\sin[(\pi/\Delta)(x-x_k)]}{x-x_k}\exp\left(-\frac{(x-x_k)^2}{2\sigma^2}\right) \\
& -2\frac{\cos[(\pi/\Delta)(x-x_k)]}{(x-x_k)^2}\exp\left(-\frac{(x-x_k)^2}{2\sigma^2}\right) \\
& -2\frac{\cos[(\pi/\Delta)(x-x_k)]}{\sigma^2}\exp\left(-\frac{(x-x_k)^2}{2\sigma^2}\right) \\
& +2\frac{\sin[(\pi/\Delta)(x-x_k)]}{(\pi/\Delta)(x-x_k)^3}\exp\left(-\frac{(x-x_k)^2}{2\sigma^2}\right) \\
& +\frac{\sin[(\pi/\Delta)(x-x_k)]}{(\pi/\Delta)(x-x_k)\sigma^2}\exp\left(-\frac{(x-x_k)^2}{2\sigma^2}\right) \\
& +\frac{\sin[(\pi/\Delta)(x-x_k)]}{(\pi/\Delta)\sigma^4}(x-x_k)\exp\left(-\frac{(x-x_k)^2}{2\sigma^2}\right) \quad (91)
\end{aligned}$$

At  $x=x_k$ , it is convenient to evaluate these derivatives separately

$$\delta_{\sigma,\Delta}^{(1)}(0) = 0 \quad (92)$$

and

$$\delta_{\sigma,\Delta}^{(2)}(0) = -\frac{1}{3}\frac{3+(\pi^2/\Delta^2)\sigma^2}{\sigma^2} \quad (93)$$

Higher order derivatives can be obtained in the same manner. Similar expressions for other DSC kernels described in the last subsection can be easily derived. The accuracy study of a few DSC kernels for fluid dynamic computations and structural analysis was given in Reference [29].

Note that the differentiation matrix in Equation (89) is generally banded. This has a distinct advantage in large scale computations. For numerical computations, it turns out that the approximate reproducing kernel has much less truncation error for interpolation and numerical differentiation. Qian and Wei [45] have recently given an estimation for truncation errors. Their estimation provides a guide to the choice of  $M$ ,  $\sigma$  and  $\Delta$ . For example, in the case of interpolation ( $n=0$ ), if the  $L_2$  norm error is set to  $10^{-\eta}$  ( $\eta>0$ ), the following relations can be deduced

$$r(\pi - B\Delta) > \sqrt{4.61\eta} \quad (94)$$

and

$$\frac{M}{r} > \sqrt{4.61\eta} \quad (95)$$

where  $r = \sigma/\Delta$  (The choice of  $\sigma$  is always proportional to  $\Delta$  so that the width of the Gaussian envelope varies with the central frequency). The first inequality states that for a given grid size  $\Delta$ , a large  $r$  is required for approximating high frequency components of an  $L^2$  function.

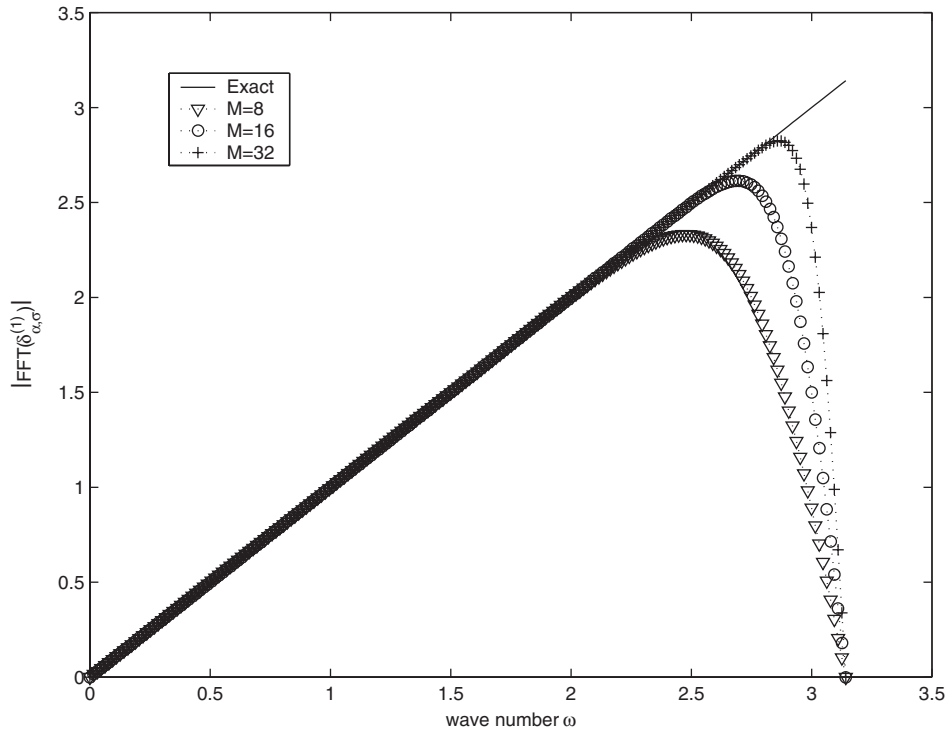


Figure 2. The discrete Fourier response of the DSC approximation to the first order derivative.

The second inequality indicates that if one chooses the ratio  $r=3$ , then the half bandwidth  $M \sim 30$  can be used to ensure the highest accuracy in a double precision computation ( $\eta=15$ ). However, for a lower accuracy requirement, a much smaller half bandwidth can be used. In general, the value of  $r$  is proportional to  $M$ . An appropriate value of  $M$  is determined by the accuracy requirement. This theoretical estimation is in excellent agreement with an earlier numerical test [46]. A discrete Fourier analysis of the DSC numerical resolution is depicted in Figure 2.

### 2.5. Methods of solution

In this subsection, we explore the unified feature of the DSC algorithm for solving differential equations. We demonstrate that in the framework of the method of weighted residuals, a few conventional computational methods, including methods of global, local, Galerkin, collocation, and finite difference, can be derived from a single starting point by using the DSC algorithm.

To solve a differential equation, one can start, either by approximating the original differential operator or by approximating the actual solution of the differential equation while maintaining the original differential operator. The latter is accomplished by explicitly defining a functional form for approximations. Let us assume that the differential equation has the general form

$$\mathcal{L}u(x) = f(x), \quad x \in \Omega \quad (96)$$

where  $\mathcal{L}$  is a linear operator and  $u(x)$  is the unknown solution of interest. Here  $f(x)$  is a known source term,  $\Omega$  denotes the domain over which the differential equation applies.

The approximate solution is sought from a finite set of  $N$  DSC ‘basis functions’ of a given resolution  $\alpha$ , denoted by  $S_{\alpha,\sigma}^{N,M}$  with  $M$  being the half width of support of each element. Here  $\sigma$  is a regularization parameter for improving the regularity of the set. The case of regularization free is easily obtained by setting  $\sigma \rightarrow \infty$ . Elements of the set  $S_{\alpha,\sigma}^{N,M}$  can be explicitly given by  $\{\phi_{\alpha,\sigma;1}^M, \phi_{\alpha,\sigma;2}^M, \dots, \phi_{\alpha,\sigma;N}^M\}$ . For a given computational domain, the resolution parameter  $\alpha$  is determined by  $N$ .

We should make use of two important properties of the DSC basis functions  $\{\phi_{\alpha,\sigma;k}^M\}$ . The first one is that when the trial function is free of regularization, each member of the set is a reproducing kernel at the highest resolution

$$\lim_{\alpha \rightarrow \infty} \langle \phi_{\alpha,\sigma;k}^M, \eta \rangle = \eta(x_k) \quad (97)$$

where  $\langle \cdot, \cdot \rangle$  denotes the standard inner product. In fact, if an appropriate basis is used for  $\phi$  and the limit on  $\sigma$  is taken,  $\phi$  of each resolution can be a reproducing kernel for  $L^2$  functions bandlimited to appropriate sense as discussed in the earlier subsections. In general, we make use of the fact that DSC kernels are good approximations to the delta distribution

$$\langle \phi_{\alpha,\sigma;k}^M, \eta \rangle \approx \eta(x_k) \quad (98)$$

This is true for appropriate  $\alpha \neq 0$ ,  $\sigma \neq 0$  and  $M \gg 0$ . The approximation in Equation (98) converges uniformly when the resolution is refined, e.g.,  $\alpha \rightarrow \infty$ . A few examples of such DSC trial functions are given in References [26, 46], and many more examples are constructed in earlier subsections. Equations (97) and (98) are special requirements satisfied by the DSC kernels of delta type [26].

The second important property of DSC trial functions is the interpolation:

$$\phi_{\alpha,\sigma;k}^M(x_j) = \delta_{kj}, \quad \forall x_k, x_j \in \Omega \quad (99)$$

Only the DSC kernels of Dirichlet type can have this interpolation property. In fact, for the purpose of numerical approximation, strict interpolation is not necessary. It was shown [46] that a quasi-interpolation scheme provides excellent computational results for solving the Fokker–Planck equation. An advantage of being interpolation is that an approximation to the function of interest  $u(x)$  can be expressed as a linear combination

$$U_{\alpha,\sigma}^{N,M}(x) = \sum_k U_{\alpha,\sigma;k} \phi_{\alpha,\sigma;k}^M(x) \quad (100)$$

where  $x$  is an independent variable and  $U_{\alpha,\sigma;k}$  is the desired DSC approximation to the solution at point  $x_k$ . The summation is over  $2M+1$  points, which are distributed around  $x$ . This structure dramatically simplifies the solution procedure in practical computations.

In this formulation, we choose the set  $S_{\alpha,\sigma}^{N,M}$  a priori, and then determine the coefficients  $\{U_{\alpha,\sigma;k}\}$  so that  $U_{\alpha,\sigma}^{N,M}(x)$  is a good approximation to  $u(x)$ . To determine  $U_{\alpha,\sigma;k}$ , we minimize the amount by which  $U_{\alpha,\sigma}^{N,M}(x)$  fails to satisfy the original governing equation (96). A measure of this discrepancy can be defined as

$$R_{\alpha,\sigma}^{N,M}(x) \equiv \mathcal{L}U_{\alpha,\sigma}^{N,M}(x) - f(x) \quad (101)$$

where  $R_{\alpha,\sigma}^{N,M}(x)$  is the residual for a particular choice of resolution, regularization and half width of the support. Note that Equation (101) is similar to the usual statement in the method of weighted residuals. However, the approximation  $U_{\alpha,\sigma}^{N,M}(x)$  is constructed by using the DSC basis functions,  $\phi_{\alpha,\sigma;k}^M(x)$ , in the present treatment. Let Equation (96) and its associated boundary conditions be well-posed, then there exists a unique solution  $u(x)$  which generally resides in an infinite-dimensional space. Since the DSC approximation  $U_{\alpha,\sigma}^{N,M}$  is constructed from a finite-dimensional set, it is generally the case that  $U_{\alpha,\sigma}^{N,M}(x) \neq u(x)$  and therefore  $R_{\alpha,\sigma}^{N,M}(x) \neq 0$ .

*Galerkin.* We seek to optimize  $R_{\alpha,\sigma}^{N,M}(x)$  by forcing it to zero in a *weighted average sense* over the domain  $\Omega$ . A convenient starting point is the Galerkin

$$\int_{\Omega} R_{\alpha,\sigma}^{N,M}(x) \phi_{\alpha',\sigma';l}^{M'}(x) dx = 0, \quad \phi_{\alpha',\sigma';l}^{M'}(x) \in S_{\alpha',\sigma'}^{N',M'} \quad (102)$$

where the weight set  $S_{\alpha',\sigma'}^{N',M'}$  can be simply chosen being identical to the DSC trial function set  $S_{\alpha,\sigma}^{N,M}$ . We refer to Equation (102) as a DSC-Galerkin statement.

*Collocation.* First, we note that in view of Equation (97), the present DSC-Galerkin statement reduces to a collocation one at the limit of  $\alpha'$

$$\lim_{\alpha' \rightarrow \infty} \int_{\Omega} R_{\alpha,\sigma}^{N,M}(x) \phi_{\alpha',\sigma';l}^{M'}(x) dx = R_{\alpha,\sigma}^{N,M}(x_l) = 0 \quad (103)$$

where  $\{x_l\}$  is the set of collocation points. However, in digital computations, we cannot take the above limit. It follows from the property of the DSC trial functions, Equation (98), that

$$\int_{\Omega} R_{\alpha,\sigma}^{N,M}(x) \phi_{\alpha',\sigma';l}^{M'}(x) dx \approx R_{\alpha,\sigma}^{N,M}(x_l) \approx 0 \quad (104)$$

It can be proven that for an appropriate choice of  $S_{\alpha',\sigma'}^{N',M'}$ , the first approximation of Equation (104) converges uniformly. The difference between the true DSC-collocation

$$R_{\alpha,\sigma}^{N,M}(x_l) = 0 \quad (105)$$

and the *Galerkin induced collocation*, (104), diminishes to zero for appropriate DSC trial functions.

*Global and local.* Global approximations to a function and its derivatives are realized typically by a set of truncated  $L^2(a,b)$  function expansions. It is called global because the values of a function and its derivatives at a particular point  $x_i$  in the coordinate space involve the *full* set of grid points in a computational domain  $\Omega$ . Whereas a local method does so by requiring only a few neighborhood points. In the present DSC approach, since the choices of  $M$  and/or  $M'$  are independent of  $N$ , one can choose  $M$  and/or  $M'$  so that a function and its derivatives at a particular point  $x_l$  are approximated either by the full set of grid points in the computational domain  $\Omega$  or just by a few grid points in the neighborhood. In fact, this freedom for the selection of  $M$  endows the DSC algorithm with *controllable accuracy* for solving differential equations and the flexibility in handling complex geometries.

A numerical demonstration of this global–local unification was given for the Euler equation under incompressible condition [27].

*Finite difference.* In the finite difference method, the differential operator is approximated by difference operations. In the present approach, the DSC-collocation expression of Equation (104) is equivalent to a  $2M + 1$  (or  $2M$ ) term finite difference method. This follows from the fact that the DSC approximation to the  $n$ th order derivative of a function can be rewritten as

$$\left. \frac{d^n u}{dx^n} \right|_{x=x_k} \approx \sum_{l=k-M}^{k+M} c_{kl,M}^n u(x_l) \quad (106)$$

where  $c_{kl,M}^n$  are a set of DSC weights for the finite difference approximation and are given by

$$c_{kl,M}^n = \left. \frac{d^n}{dx^n} \phi_{\alpha,\sigma;l}^M(x) \right|_{x=x_k} \quad (107)$$

Here,  $\{x_k\}$  are chosen centered around the  $x_l$ . Note that the standard finite difference scheme is obtained if  $\phi_{\alpha,\sigma;l}^M$  is chosen as the Lagrange kernel

$$L_{M,l}(x) = \prod_{i=l-M, i \neq l}^{i=l+M} \frac{x - x_i}{x_l - x_i}, \quad (M \geq 1)$$

where  $\alpha \propto 1/\Delta$  and the parameter  $\sigma$  does not apply since the kernel is not regularized. Obviously, for each different choice of  $\phi_{\alpha,\sigma}^M$ , we have a different DSC-finite difference approximation. Hence, the present DSC approach is a generalized finite difference method. This DSC-finite difference was tested in previous studies [46]. When  $M=1$ , the DSC-finite difference approximation reaches its lowest order limit and the resulting matrix is tridiagonal. In this case, by appropriately choosing the parameter  $\sigma$ , the present DSC weights  $c_{kl,M}^q$  can always be made exactly the same as those of the standard second order central difference scheme, i.e.  $1/2\Delta$ ,  $0$ ,  $-1/2\Delta$  for the first order derivative and  $1/\Delta^2$ ,  $-2/\Delta^2$ ,  $1/\Delta^2$  for the second order derivative. Here  $\Delta$  is the grid spacing. However, for a given numerical bandwidth, the DSC-finite difference approximation does not have to be the same as the standard finite difference scheme and can be optimized in a practical application by varying  $\sigma$ . Another important choice of the DSC bandwidth is that  $M=N$ , where  $N$  is the matrix length. Obviously, the computational matrix is no longer banded and this is a case we called a ‘global finite difference method’.

It is noted that if the DSC kernels of positive type are used, the DSC trial function, Equation (100), needs to be constructed in a more general manner. Such a change does affect the deduction of collocation from the DSC Galerkin and the unified feature between the global and the local. However, the generalized finite difference schemes cannot be deduced.

### 3. ANALYSIS OF PLATES

In this section, the treatment of plate vibrations by using the DSC algorithm is discussed. Although we limit our attention to the vibration of rectangular (classic) Kirchhoff plates with simply supported, clamped and transversely supported edges, the method can be used for

many other applications of solid mechanics. Let us consider a rectangular plate which has a length  $a$ , width  $b$ , thickness  $h$ , mass density  $\rho$ , modulus of elasticity  $E$ , and Poisson's ratio  $\nu$ . The governing differential equation for the plate is given by [47]

$$\frac{\partial^4 w}{\partial x^4} + 2 \frac{\partial^4 w}{\partial x^2 \partial y^2} + \frac{\partial^4 w}{\partial y^4} = \frac{\rho h \omega^2}{D} w \quad (108)$$

where  $w(x, y)$  is the transverse displacement of the midsurface of the plate,  $D = Eh^3/[12(1 - \nu^2)]$  the flexural rigidity, and  $\omega$  the circular frequency. We consider one of the following three types of support conditions for each plate edge:

For simply supported edge (S):

$$w = 0, \quad -D \left( \frac{\partial^2 w}{\partial n^2} + \nu \frac{\partial^2 w}{\partial s^2} \right) = 0 \quad (109)$$

For clamped edge (C):

$$w = 0, \quad \frac{\partial w}{\partial n} = 0 \quad (110)$$

For transversely supported edge with nonuniform elastic rotational restraint (E):

$$w = 0, \quad -D \left( \frac{\partial^2 w}{\partial n^2} + \nu \frac{\partial^2 w}{\partial s^2} \right) = K(s) \frac{\partial w}{\partial n} \quad (111)$$

where  $K(s)$  is the varying elastic rotational stiffness of the plate elastic edge and  $n$  and  $s$  denote, respectively, the normal and tangential coordinates with respect to the rectangular plate edge.

For generality and simplicity, the following dimensionless parameters are introduced:

$$X = \frac{x}{a}, \quad Y = \frac{y}{b}, \quad W = \frac{w}{a}; \quad \lambda = \frac{a}{b}; \quad \Omega = \omega a^2 \sqrt{\frac{\rho h}{D}} \quad (112)$$

Accordingly, we obtain the dimensionless governing equation for the vibration analysis of a rectangular plate as:

$$\frac{\partial^4 W}{\partial X^4} + 2\lambda^2 \frac{\partial^4 W}{\partial X^2 \partial Y^2} + \lambda^4 \frac{\partial^4 W}{\partial Y^4} = \Omega^2 W \quad (113)$$

Consider a uniform grid having

$$0 = X_0 < X_1 < \dots < X_{N_X} = 1$$

and

$$0 = Y_0 < Y_1 < \dots < Y_{N_Y} = 1$$

To formulate the eigenvalue problem, we introduce a column vector  $\mathbf{W}$  as

$$\mathbf{W} = (W_{0,0}, \dots, W_{0,N_Y}, W_{1,0}, \dots, W_{N_X,N_Y})^T \quad (114)$$

with  $(N_X + 1)(N_Y + 1)$  entries  $W_{i,j} = W(X_i, Y_j)$ , ( $i = 0, 1, \dots, N_X$ ;  $j = 0, 1, \dots, N_Y$ ).

Let us define the  $(N_q + 1) \times (N_q + 1)$  differentiation matrices  $\mathbf{D}_q^n$  ( $q = X, Y; n = 1, 2, \dots$ ), with their elements given by

$$[\mathbf{D}_q^n]_{i,j} = \delta_{\sigma,\Delta}^{(n)}(q_i - q_j), \quad (i, j = 0, \dots, N_q) \tag{115}$$

where  $\delta_{\sigma,\Delta}(q_i - q_j)$  is a DSC kernel of delta type [26]. Here  $\Delta$  is the grid spacing and  $\sigma$  determines the effective computational bandwidth. Many DSC kernels were constructed in the original work. Here, we choose a simple example, the regularized Shannon’s delta kernel  $\delta_{\sigma,\Delta}(q - q_j) = \sin [(\pi/\Delta)(q - q_j)] / [(\pi/\Delta)(q - q_j)] e^{-(q - q_j)^2 / (2\sigma^2)}$ , to illustrate the algorithm and its application. Other DSC kernels, such as the regularized Dirichlet kernel and regularized Lagrange kernel, can also be used. The performance of a few DSC kernels for fluid dynamic computations and structural analysis was compared in Reference [33]. As mentioned already, the differentiation in Equation (115) can be *analytically* carried out

$$\delta_{\sigma,\Delta}^{(n)}(q_i - q_j) = \left[ \left( \frac{d}{dq} \right)^n \delta_{\sigma,\Delta}(q - q_j) \right]_{q=q_i} = C_m^n \tag{116}$$

where, for a uniform grid spacing,  $m = (q_i - q_j) / \Delta$ . Here the matrix is banded to  $i - j = m = -M, \dots, 0, \dots, M$ . Therefore, the system of linear algebraic equations for the governing PDE (113) is given by

$$(\mathbf{D}_X^4 \otimes \mathbf{I}_Y + 2\lambda^2 \mathbf{D}_X^2 \otimes \mathbf{D}_Y^2 + \lambda^4 \mathbf{I}_X \otimes \mathbf{D}_Y^4) \mathbf{W} = \Omega^2 \mathbf{W} \tag{117}$$

where  $\mathbf{I}_q$  is the  $(N_q + 1) \times (N_q + 1)$  unit matrix and  $\otimes$  denotes the tensorial product. Eigenvalues can be evaluated from Equation (117) by using a standard solver. However, appropriate boundary conditions are to be implemented before calculating eigenvalues. This is described below.

We first note that boundary condition  $W = 0$  is easily specified at the edge. To implement other boundary conditions, we assume, for a function  $f$ , the following relation between the inner nodes and the outer nodes on the left boundary

$$f(X_{-m}) - f(X_0) = \left( \sum_{j=0}^J a_m^j X_m^j \right) [f(X_m) - f(X_0)] \tag{118}$$

where coefficients  $a_m^j$  ( $m = 1, \dots, M, j = 0, 1, \dots, J$ ) are to be determined by the boundary conditions. For the three types of boundary conditions described earlier, we only need to consider the zeroth order term in the power of  $X^j$ . Therefore we set  $a_m^0 \equiv a_m$  and, after rearrangement, obtain

$$f(X_{-m}) = a_m f(X_m) + (1 - a_m) f(X_0), \quad m = 1, 2, \dots, M \tag{119}$$

According to Equation (116), the first and the second derivatives of  $f$  on the boundary are approximated by

$$f'(X_0) = \sum_{m=-M}^M C_m^1 f(X_m) \tag{120}$$

$$= \left[ C_0^1 - \sum_{m=1}^M (1 - a_m) C_m^1 \right] f(X_0) + \sum_{m=1}^M (1 - a_m) C_m^1 f(X_m) \tag{121}$$

and

$$f''(X_0) = \sum_{m=-M}^M C_m^2 f(X_m) = \left[ C_0^2 + \sum_{m=1}^M (1 - a_m) C_m^2 \right] f(X_0) + \sum_{m=1}^M (1 + a_m) C_m^2 f(X_m)$$

respectively.

For simply supported edges, the boundary conditions reduce to

$$f(X_0) = 0, \quad f''(X_0) = 0 \tag{122}$$

These are satisfied by choosing  $a_m = -1, m = 1, 2, \dots, M$ . This is the so-called *anti-symmetric extension* [26].

For clamped edges, the boundary conditions require

$$f(X_0) = 0, \quad f'(X_0) = 0 \tag{123}$$

These are satisfied by  $a_m = 1, m = 1, 2, \dots, M$ . This is the *symmetric extension* [26].

For a transversely supported edge, the boundary conditions are

$$f(X_0) = 0, \quad f''(X_0) - Kf'(X_0) = 0 \tag{124}$$

Hence, the equation is given by

$$\sum_{m=1}^M (1 + a_m) C_m^2 f(X_m) - K \sum_{m=1}^M (1 - a_m) C_m^1 f(X_m) = 0 \tag{125}$$

Further simplification of the above equation gives

$$\sum_{m=1}^M [(1 + a_m) C_m^2 - K(1 - a_m) C_m^1] f(X_m) = 0 \tag{126}$$

One way to satisfy Equation (126) is to choose

$$a_m = \frac{KC_m^1 - C_m^2}{KC_m^1 + C_m^2}, \quad m = 1, 2, \dots, M \tag{127}$$

Expressions for the right, top and bottom boundaries can be derived in a similar way.

Further complication occurs if the coefficient  $K$  is not a constant. For example, the rotational spring coefficients  $K_1(Y), K_2(Y), K_3(X)$  and  $K_4(X)$  are taken as

$$K_1(Y) = K_2(Y) = K'Y(1 - Y) \tag{128}$$

$$K_3(X) = K_4(X) = K'X(1 - X)/\lambda \tag{129}$$

where  $K'$  is the nondimensional spring coefficient,  $K' = K_0 a^3 / D$ . Another complication is due to the possible presence of irregular internal support condition. Hence, matrices  $\mathbf{D}_X^4, \mathbf{D}_Y^4, \mathbf{D}_X^2, \mathbf{D}_Y^2, \mathbf{I}_X$  and  $\mathbf{I}_Y$  become three-dimensional ones in this work and are denoted by  $\mathcal{D}_X^4, \mathcal{D}_Y^4, \mathcal{D}_X^2, \mathcal{D}_Y^2, \mathcal{I}_X$  and  $\mathcal{I}_Y$ . The matrix elements of  $\mathcal{D}_X^p, (p = 2, 4)$  are denoted by  $d_{X,ijk}^p, (i, j = 0, 1, 2, \dots, N_X;$

$k = 0, 1, 2, \dots, N_Y$ ) and matrix elements of  $\mathcal{I}_X$  is denoted by  $\delta_{ij} \otimes 1_k$ , ( $k = 0, 1, 2, \dots, N_Y$ ).  $\mathcal{D}_Y^p$  and  $\mathcal{I}_Y$  are similarly defined by appropriately switching the roles of the subscripts.

Let us define a contractive tensor product  $\dot{\otimes}$  of two three-dimensional matrices  $\mathcal{A}$  and  $\mathcal{B}$  as the tensor product on the first two indices of  $\mathcal{A}$  and  $\mathcal{B}$ , and contraction between the first and the third indices of the two matrices

$$(\mathcal{A} \dot{\otimes} \mathcal{B})_{i \times N_y + k, j \times N_y + l} = a_{ijk} b_{kli} \tag{130}$$

where  $a_{ijk}$  and  $b_{kli}$  are matrix elements of  $\mathcal{A}$  and  $\mathcal{B}$ , respectively. In such a notation, Equation (117) is modified as

$$(\mathcal{D}_X^4 \dot{\otimes} \mathcal{I}_Y + 2\lambda^2 \mathcal{D}_X^2 \dot{\otimes} \mathcal{D}_Y^2 + \lambda^4 \mathcal{I}_X \dot{\otimes} \mathcal{D}_Y^4) \mathbf{W} = \Omega^2 \mathbf{W} \tag{131}$$

where the lexicographic ordering given in Equation (114) is used for reducing four-dimensional matrices into two-dimensional forms. Matrix elements in Equation (131) are ready for being used in a linear equation solver

$$\mathcal{I}_X \dot{\otimes} \mathcal{D}_Y^4 = \begin{pmatrix} d_{Y,000}^4 & d_{Y,010}^4 & \cdots & 0 & 0 & \cdots \\ d_{Y,100}^4 & d_{Y,110}^4 & \cdots & 0 & 0 & \cdots \\ \vdots & \vdots & \ddots & \vdots & \vdots & \ddots \\ 0 & 0 & \cdots & d_{Y,001}^4 & d_{Y,011}^4 & \cdots \\ 0 & 0 & \cdots & d_{Y,101}^4 & d_{Y,111}^4 & \cdots \\ \vdots & \vdots & \ddots & \vdots & \vdots & \ddots \\ \vdots & \vdots & & \vdots & \vdots & \ddots \end{pmatrix}$$

$$\mathcal{D}_X^4 \dot{\otimes} \mathcal{I}_Y = \begin{pmatrix} d_{X,000}^4 & 0 & \cdots & 0 & d_{X,010}^4 & 0 & \cdots & 0 \\ 0 & d_{X,001}^4 & \cdots & 0 & 0 & d_{X,011}^4 & \cdots & 0 \\ \vdots & & \ddots & \vdots & \vdots & & \ddots & \vdots \\ 0 & \cdots & \cdots & d_{X,00N_Y}^4 & 0 & \cdots & \cdots & d_{X,01N_Y}^4 \\ d_{X,100}^4 & 0 & \cdots & 0 & d_{X,110}^4 & 0 & \cdots & 0 \\ 0 & d_{X,101}^4 & \cdots & 0 & 0 & d_{X,111}^4 & \cdots & 0 \\ \vdots & & \ddots & \vdots & \vdots & & \ddots & \vdots \\ 0 & \cdots & \cdots & d_{X,10N_Y}^4 & 0 & \cdots & \cdots & d_{X,11N_Y}^4 \\ \vdots & & & \vdots & \vdots & & & \ddots \end{pmatrix}$$

and

$$\mathcal{D}_x^2 \otimes \mathcal{D}_y^2 = \left( \begin{array}{ccc|ccc|c} d_{x,000}^2 d_{y,000}^2 & d_{x,000}^2 d_{y,010}^2 & \cdots & d_{x,010}^2 d_{y,000}^2 & d_{x,010}^2 d_{y,010}^2 & \cdots & \\ d_{x,001}^2 d_{y,100}^2 & d_{x,001}^2 d_{y,110}^2 & \cdots & d_{x,011}^2 d_{y,100}^2 & d_{x,011}^2 d_{y,110}^2 & \cdots & \cdots \\ \vdots & \vdots & \ddots & \vdots & \vdots & \ddots & \\ \hline d_{x,100}^2 d_{y,001}^2 & d_{x,100}^2 d_{y,011}^2 & \cdots & d_{x,110}^2 d_{y,001}^2 & d_{x,110}^2 d_{y,011}^2 & \cdots & \\ d_{x,101}^2 d_{y,101}^2 & d_{x,101}^2 d_{y,111}^2 & \cdots & d_{x,111}^2 d_{y,101}^2 & d_{x,111}^2 d_{y,111}^2 & \cdots & \cdots \\ \vdots & \vdots & \ddots & \vdots & \vdots & \ddots & \\ \hline & \vdots & & & \vdots & & \ddots \end{array} \right)$$

Assume that the set of internal support points are given by  $\{(X_{i'}, Y_{j'})\}$ , the internal support conditions ( $W_{i,j} = 0, \forall (X_i, Y_j) \in \{(X_{i'}, Y_{j'})\}$ ) are specified pointwisely in the matrix construction.

#### 4. CONCLUSION

In conclusion, a novel numerical approach, the DSC method, is developed for vibration analysis of rectangular plates with partial internal line or point supports. The computational philosophy of the DSC algorithm is studied. Many sequences of approximations to the delta distribution, the 'universal reproducing kernel', are constructed either as bandlimited reproducing kernels or as approximate reproducing kernels. A regularization procedure based on the distribution theory is utilized to improve the regularity and localization of the DSC kernels. Systematic treatments of derivatives and boundary conditions are proposed, as they are required for a computational algorithm.

We explore the unified features of DSC algorithm for solving differential equations in the framework of the method of weighted residuals. It is found that several computational methods, such as global, local, Galerkin, collocation and finite difference methods, can be derived from a single starting point by using DSC trial functions and test functions. The unification of local and global methods is realized via the DSC approach. It is well known that accuracy is crucial to many scientific computations, such as simulation of turbulence, analysis of an entire radar cross-section and frequency parameters of higher order vibration modes. Whereas, small-matrix-band approximations are vital to large scale computations. The DSC approach provides a controllable numerical accuracy by an appropriate selection of the matrix bandwidth. Therefore, by using the DSC algorithm, the computational efficiency can be easily optimized against accuracy, convergence, stability and simplicity. A collocation algorithm is deduced from a Galerkin statement and is called a Galerkin-induced collocation. The equivalence of Galerkin and collocation enables us to evaluate these two conventional numerical algorithms on an equal footing. The connection is made between finite difference and other methods, such as collocation and Galerkin. The DSC algorithm can be regarded as a generalized finite difference method, which becomes a 'global finite difference method'

by an appropriate choice of the computational bandwidth. These results can be used as a guide for the selection of computational methods and for the design of numerical solvers for practical applications. The application emphasized in this work is vibration analysis of rectangular plate with internal supports. Both partial line support and complex internal are considered to illustrate the proposed algorithm in Part 2.

As a summary for the computational method proposed for vibration analysis, we conclude the following remarks for the DSC algorithm:

- (i) Like a wavelet basis function, kernels of DSC algorithm usually have time-frequency localization. In fact, the commonly used DSC kernels, such as the regularized Shannon's kernel and regularized Lagrange kernel, have controllable bandwidth in both the co-ordinate domain and the frequency domain. As a consequence, they have controllable accuracy and computational bandwidths for numerical computations. If it is desirable to save computing time in a large-scale computation, the effective support of the DSC kernel can be reduced by choosing a smaller bandwidth parameter. On the other hand, if the accuracy is of great importance for a particular application, the computational bandwidth can be appropriately enlarged to meet the accuracy requirement. Both the global limit and the low order finite difference limit can be easily reached in the DSC algorithm by an appropriate selection of parameters [27].
- (ii) By using the fictitious domain, complex boundary conditions which occur in plate analysis can be treated without any additional computational effort. In fact, unlike most conventional methods, the DSC algorithm is designed to satisfy the boundary conditions even at the continuous limit.
- (iii) Since most commonly used DSC kernels are either interpolation or quasi-interpolation type, the expansion coefficient for each 'basis function' at a spatial location is the value of the solution at the same location. Hence, no additional integration is required for determining expansion coefficients.
- (iv) Since the DSC kernels are approximations to the delta distributions, the Galerkin and collocation become essentially equivalent when the DSC parameters are appropriately chosen. Therefore, the time-consuming integration procedure required in the Galerkin and/or Rayleigh-Ritz methods is no longer needed in the DSC algorithm.
- (v) Owing to numerical round off errors, most spectral methods become unstable when the order of the approximation is increased to a certain level. In contrast, DSC algorithm remains very stable when the number of DSC basis functions increases. The total number of basis functions can be chosen as large as one wishes and is limited only by the computer memory and speed.
- (vi) Many DSC kernels are functions of the Schwartz class or certain high regularity functions. They can be used for the optimal design of conjugated filters. Conjugated filters are a set of low-pass and band-(high-) pass filters that are derived from a single starting point, and have essentially the same time-frequency localization, regularity, frequency band, and effective support. The DSC conjugate filters are particularly efficient for the elimination of spurious oscillations (Gibbs phenomena) which occur in solving problems of nonlinear hyperbolic conservation law and compressible fluid flow. In fact, the DSC theory provides a unified description to solution of partial differential equations and image/signal processing.

## ACKNOWLEDGEMENT

This work was supported by the National University of Singapore and by the University of Western Sydney.

## REFERENCES

1. Chladni EFF. *Entdeckungen uber die Theorie des Klanges*. Leipzig, 1787.
2. Leissa AW. Recent research in plate vibrations: classic theory. *Shock and Vibration Digest* 1977; **9**(10):13–24.
3. Leissa AW. Recent research in plate vibrations: complicating effects. *Shock and Vibration Digest* 1977; **9**(11):21–35.
4. Leissa AW. Plate vibration research: 1976–1981: classic theory. *Shock and Vibration Digest* 1981; **13**(9):11–22.
5. Leissa AW. Plate vibration research: 1976–1981: complicating effects. *Shock and Vibration Digest* 1981; **13**(10):19–36.
6. Leissa AW. Recent research in plate vibrations: 1981–1985: Part I. Classic theory. *Shock and Vibration Digest* 1987; **19**(2):11–18.
7. Leissa AW. Recent research in plate vibrations: 1981–1985: Part II. Complicating effects. *Shock and Vibration Digest* 1987; **19**(3):10–24.
8. Leissa AW. *Vibration of Plates*. NASA SP-160. Office of Technology Utilization, NASA: Washington, DC, 1969.
9. Liew KW, Wang CM, Xiang Y, Kitipornchai S. *Vibration of Mindlin Plates*. Elsevier Science: Oxford, UK, 1998.
10. Veletsos AS, Newmark NM. Determination of natural frequencies of continuous plates hinged along two opposite edges. *Journal of Applied Mechanics* 1956; **23**:97–102.
11. Ungar EE. Free oscillations of edge-connected simply supported plate systems. *Journal of Engineering for Industry* 1961; **83**:434–440.
12. Bolotin VV. A generalization of the asymptotic method of the eigenvalue problems for rectangular regions (in Russian). *Inzhenernyi Zhurnal* 1961; **3**:86–92.
13. Moskalenko VN, De-Lin Chen. On the natural vibrations of multispan plates (in Russian). *Prikladnaya Mekhanika* 1965; **1**:59–66.
14. Cheung YK, Cheung MS. Flexural vibrations of rectangular and other polygonal plates. *Journal of the Engineering Mechanics Division, American Society of Civil Engineers* 1971; **97**:391–411.
15. Elishakoff I, Sternberg A. Eigenfrequencies of continuous plates with arbitrary number of equal spans. *Journal of Applied Mechanics* 1979; **46**:656–662.
16. Azimi A, Hamilton JF, Soedel W. The receptance method applied to the free vibration of continuous rectangular plates. *Journal of Sound and Vibration* 1984; **93**:9–29.
17. Mizusawa T, Kajita T. Vibration of continuous skew plates. *Earthquake Engineering and Structural Dynamics* 1984; **12**:847–850.
18. Takahashi K, Chishaki T. Free vibrations of two-way continuous rectangular plates. *Journal of Sound and Vibration* 1979; **62**:455–459.
19. Wu CI, Cheung YK. Frequency analysis of rectangular plates continuous in one or two directions. *Earthquake Engineering and Structural Dynamics* 1974; **3**:3–14.
20. Kim CS, Dickinson SM. The flexural vibration of line supported rectangular plate systems. *Journal of Sound and Vibration* 1987; **114**:129–142.
21. Liew KM, Lam KY. Vibration analysis of multi-span plates having orthogonal straight edges. *Journal of Sound and Vibration* 1991; **147**:255–264.
22. Liew KM, Xiang Y, Kitipornchai S. Transverse vibration of thick rectangular plates—II. Inclusion of oblique internal line supports. *Computers and Structures* 1993; **49**:31–58.
23. Zhou D. Eigenfrequencies of line supported rectangular plates. *International Journal of Solids and Structures* 1994; **31**:347–358.
24. Kong J, Cheung YK. Vibration of shear-deformable plates with intermediate line supports: a finite layer approach. *Journal of Sound and Vibration* 1995; **184**:639–649.
25. Liew KM, Wang CM. Vibration of triangular plates-point supports, mixed edges and partial internal curved supports. *Journal of Sound and Vibration* 1994; **172**(4):527–537.
26. Wei GW. Discrete singular convolution for the solution of the Fokker–Planck equations. *Journal of Chemical Physics* 1999; **110**:8930–8942.
27. Wei GW. A unified approach for the solution of the Fokker–Planck equations. *Journal of Physics A* 2000; **33**:4935–4953.
28. Wei GW. Wavelets generated by the discrete singular convolution kernels. *Journal of Physics A* 2000; **33**:8577–8596.

29. Wei GW. A new algorithm for solving some mechanical problems. *Computer Methods in Applied Mechanics and Engineering* 2001; **190**:2017–2030.
30. Schwartz L. *Théorie des Distributions*, Hermann: Paris, 1951.
31. Wei GW. Solving quantum eigenvalue problems by discrete singular convolution. *Journal of Physics B* 2000; **33**:343–352.
32. Wan DC, Patnaik BSV, Wei GW. Discrete singular convolution-finite subdomain method for the solution of incompressible flows. *Journal of Computational Physics* 2002; **180**:1–27.
33. Wei GW. A unified method for computational mechanics. In *Computational Mechanics for the Next Millennium*, Wang CM, Lee KH, Ang KK, (eds). Amsterdam: Elsevier, 1999; 1049–1054.
34. Zhao YB, Wei GW. DSC Analysis of rectangular plates with nonuniform boundary conditions. *Journal of Sound and Vibration*, in press.
35. Wei GW. Generalized Perona–Malik equation for image restoration. *IEEE Signal Processing Letters* 1999; **6**:165–168.
36. Wei GW. Discrete singular convolution method for the sine-Gordon equation. *Physica D* 2000; **137**:247–259.
37. Ablowitz MJ, Herbst BM, Schober C. On numerical solution of the sine-Gordon equation. *Journal of Computational Physics* 1996; **126**:299–314.
38. Guan S, Lai C-H, Wei GW. Fourier-Bessel characterizations of patterns in a circular domain. *Physica D* 2001; **151**:83–98.
39. Korevaar J. *Mathematical Methods*, vol. 1. Academic Press: New York, 1968.
40. Walter GG, Blum J. Probability density estimation using delta sequences. *Annals of Statistics* 1977; **7**:328–340.
41. Winter BB. Rate of strong consistency of two nonparametric density estimators. *Annals of Statistics* 1975; **3**:759–766.
42. Wahba G. Optimal convergence properties of variable knot, kernel, and orthogonal series methods for density estimation. *Annals of Statistics* 1975; **3**:15–29.
43. Kronmal R, Tarter M. The estimation of probability density and cumulatives by Fourier series methods. *Journal of the American Statistical Association* 1968; **63**:925–952.
44. Bohm A. *Quantum Mechanics* (3rd edn). Springer: Berlin, 1993.
45. Qian LW, Wei GW. A note on regularized Shannon’s sampling formulae. *Preprint* arXiv:math.SC/0005003, 2000.
46. Wei GW. Quasi wavelets and quasi interpolating wavelets. *Chemical Physics Letters* 1998; **296**:215–222.
47. Timoshenko SP, Woinowsky-Krieger S. *Theory of Plates and Shells*. McGraw-Hill: Singapore, 1970.